Polymer 49 (2008) 2046–2054

Contents lists available at ScienceDirect

Polymer

journal homepage: www.elsevier.com/locate/polymer

Superporous poly(2-hydroxyethyl methacrylate) based scaffolds: Preparation and characterization

D. Horák *, H. Hlídková, J. Hradil, M. Lapčíková, M. Šlouf

Institute of Macromolecular Chemistry, Academy of Sciences of the Czech Republic, v.v.i., Heyrovský Sq. 2, 162 06 Prague 6, Czech Republic

ARTICLE INFO

Article history:
Received 14 December 2007
Received in revised form 18 February 2008
Accepted 25 February 2008
Available online 4 March 2008

Keywords:
2-Hydroxyethyl methacrylate
Scaffold
Porosity

ABSTRACT

Superporous poly(2-hydroxyethyl methacrylate) (PHEMA) scaffolds with pore size from 10^1 to 10^2 μm range were prepared by radical polymerization of 2-hydroxyethyl methacrylate (HEMA) with 2 wt.% ethylene dimethacrylate (EDMA) with the aim to obtain a support for cell cultivation. Superpores were formed by salt-leaching technique using NaCl or $(NH_4)_2SO_4$ as a porogen. Addition of liquid porogen (cyclohexanol/dodecan-1-ol (CyOH/DOH) = 9/1 w/w) to the polymerization mixture did not substantially affect the formation of meso- and macropores. The prepared slabs were characterized by several methods including water and cyclohexane regain by centrifugation, water regain by suction, scanning electron microscopy (SEM), mercury porosimetry and dynamic desorption of nitrogen. High-vacuum scanning electron microscopy (HVSEM) confirmed permeability of hydrogel slabs to 8-μm microspheres, whereas low-vacuum scanning electron microscopy (LVSEM) at cryo-conditions showed the undeformed structure of the frozen slabs. Interconnection of pores in the PHEMA slabs was proved. Water regain estimated by centrifugation method did not include volume of large superpores (imprints of porogen crystals), in contrast to water regain by suction method. The porosities of the slabs ranging from 81 to 91% were proportional to the volume of porogen in the feed.

1. Introduction

Polymer scaffolds have received much attention as microenvironment for cell adhesion, proliferation, migration and differentiation in tissue engineering and regenerative medicine. The three-dimensional scaffold structure provides support for high level of tissue organization and remodelling. Regeneration of different tissues, such as bone [1], cartilage [2], skin [3], nerves [4], or blood vessels [5], is investigated using such supports. An ideal polymer scaffold should thus mimic the living tissue, i.e. possess a high water content, which could possibly incorporate bioactive molecules allowing a better control of cell differentiation. At the same time it requires a range of properties including biocompatibility and/or biodegradability, highly porous structure with communicating pores allowing high cell adhesion and tissue in-growth. The material should be sterilizable and also possess good mechanical strength. Both natural and synthetic scaffolds are being developed. The advantage of synthetic polymer matrices consists in their easy processability, tunable physical and chemical properties, susceptibility to modifications and possibly controlled degradation.

Many techniques have been developed to fabricate highly porous scaffolds for tissue engineering. They include for instance solvent casting [6], gas foaming [7] and/or salt-leaching [8], freeze–thaw procedure [9,10], supercritical fluid technology [11] (disks exposed to CO_2 at high pressure) and electrospinning (for nanofibre matrices) [12]. A wide range of polymers were suggested for scaffolds. In addition to natural materials, such as collagen, gelatin, dextran [13], chitosan [14], phosphorylcholine [15], alginic [16] and hyaluronic acids, it includes also synthetic polymers, e.g., poly(vinyl alcohol) [17], poly(lactic acid) [1,18], polycaprolactone [19], poly(ethylene glycol) [20], polyacrylamide [21], polyphosphazenes [22], as well as polyurethane [23].

Among various kinds of materials being used in biomedical and pharmaceutical applications, hydrogels composed of hydrophilic polymers or copolymers find a unique place. They have a highly water-swollen rubbery three-dimensional structure which is similar to natural tissue [24,25]. In this paper, poly(2-hydroxyethyl methacrylate) (PHEMA) was selected as the hydrogel for a potential scaffold intended for cell cultivation. The presence of hydroxy and carboxy groups makes this polymer compatible with water, whereas the hydrophobic methyl groups and backbone impart hydrolytic stability to the polymer and support the mechanical strength of the matrix [26]. PHEMA hydrogels are known for their

* Corresponding author. Institute of Macromolecular Chemistry, Academy of Sciences of the Czech Republic, Department of Bioanalogous and Special Polymers, Heyrovský Sq. 2, 162 06 Prague 6, Czech Republic. Tel.: +420 296 809 260; fax: +420 296 809 410.
E-mail address: horak@imc.cas.cz (D. Horák).

0032-3861/$ – see front matter © 2008 Elsevier Ltd. All rights reserved.
doi:10.1016/j.polymer.2008.02.041

resistance to high temperatures, acid and alkaline hydrolysis and low reactivity with amines [27]. Previously, porous structure in PHEMA slabs was obtained by phase separation using a low-molecular weight or polymeric porogen, or by the salt-leaching method. The material was used as a mouse embryonic stem cell support [8,28,29]. The aim of this paper is to demonstrate conditions under which communicating pores are formed enabling high permeability of PHEMA scaffolds which is crucial for future cell seeding.

2. Experimental

2.1. Reagents

2-Hydroxyethyl methacrylate (HEMA, Röhm GmbH, Germany) and ethylene dimethacrylate (EDMA, Ugilor S.A., France) were purified by distillation. 2,2′-Azobisisobutyronitrile (AIBN, Fluka) was crystallized from ethanol and used as initiator. Sodium chloride G.R. (Lach-Ner, s.r.o. Neratovice, Czech Republic) was classified, particle size 250–500 μm and ammonium sulfate needles (100 × 600 μm, Lachema, Neratovice, Czech Republic) were used as porogens. Cyclohexanol (CyOH, Lachema, Neratovice, Czech Republic) was distilled; dodecan-1-ol (DOH) and all other solvents and reagents were obtained from Aldrich and used without purification. Ammonolyzed PGMA microspheres (2 μm) were obtained by the previously described procedure [30]. Sulfonated polystyrene (PSt) microspheres (8 μm) Ostion LG KS 0803 were purchased from Spolek pro chemickou a hutní výrobu, Ústí n. L., Czech Republic. Polyaniline hydrochloride microspheres (PANI, 200–400 nm) were prepared according to literature [31].

2.2. Slab preparation

Crosslinked hydrogel slabs were prepared by the bulk radical polymerization of a reaction mixture containing monomer (HEMA), crosslinking agent (EDMA), initiator (AIBN) and NaCl and/or liquid diluent as a porogen (CyOH/DOH = 9/1 w/w). The compositions of polymerization mixtures are summarized in Table 1. The amount of crosslinker (2 wt.%) and AIBN (1 wt.%) in monomers was the same in all experiments, while the amount of an inorganic salt in the polymerization feed, such as NaCl used as a porogen, was varied from 35.9 to 41.4 vol.%. Optionally, needle-like $(NH_4)_2SO_4$ crystals (42.3 vol.%) together with saturated $(NH_4)_2SO_4$ solution were used as a porogen instead of NaCl crystals. The needle-like shape of crystals was convenient for the preparation of slabs with communicating pores (Run 9, Table 1). For the sake of comparison, a copolymer was prepared with a mixture of solid (NaCl) and liquid low-molecular weight porogen (diluent) (Run 8). The content of liquid porogen (diluent) amounted to 50% of the polymerization feed. The thickness of the slab was adjusted with a 3-mm thick silicone rubber spacer between the Teflon plates (10 × 10 cm), which were greased with a silicone oil and covered with Cellophane to facilitate removal of the sheet after polymerization. The reaction mixture was transferred onto a plate and covered with a second plate. The two plates were clamped and heated in a bath at 70 °C for 8 h. After polymerization, the slabs obtained with NaCl or $(NH_4)_2SO_4$ as a porogen were soaked in water and washed until the reaction of chloride or sulfate ions disappeared. The slabs prepared in the presence of a liquid diluent were washed with ethanol/water mixtures (98/2, 70/30, 40/60, 10/90 v/v) and water to remove the diluent, unreacted monomers and initiator residues. The washing water was then changed every day for 2 weeks.

Table 1
Preparation of PHEMA slabs, conditions and properties[a]

Run	NaCl (vol.%)	Water regain (ml/g)		CX regain[d] (ml/g)	Cumulative pore volume[f] (ml/g)
1	41.4	0.84[d]	7.52[e]	0.13	0.35
2	40.8	0.88[d]	7.40[e]	0.23	0.47
3	40.0	1.04[d]	5.34[e]	0.56	1.03
4	39.1	0.81[d]	4.05[e]	0.33	1.24
5	37.9	0.78[d]	4.04[e]	0.21	1.60
6	37.0	0.79[d]	3.64[e]	0.34	1.83
7	35.9	0.75[d]	3.32[e]	0.32	1.70
8[b]	37.9	0.89[d]	4.30[e]	0.45	1.65
9	42.3[c]	0.84[d]	2.11[e]	0.08	0.08

[a] Crosslinked with 2 wt.% EDMA, 1 wt.% AIBN, NaCl in vol.% relative to polymerization mixture (HEMA + EDMA + NaCl).
[b] One half of the HEMA/EDMA feed was replaced by CyOH/DOH = 9/1 w/w.
[c] $(NH_4)_2SO_4$.
[d] Centrifugation method.
[e] Suction method.
[f] Mercury porosimetry.

2.3. Methods

2.3.1. Microscopy

Low-vacuum scanning electron microscopy (LVSEM) was performed with a microscope Quanta 200 FEG (FEI, Czech Republic). Neat hydrated hydrogel slabs were cut with a razor blade into ~5-mm cubes, flash-frozen in liquid nitrogen and placed on the sample stage cooled to −10 °C. Before microscopic observation, the top of a frozen sample was cut off using a sharp blade. During the observation, the conditions in the microscope (−10 °C, 100 Pa) caused slow sublimation of ice from the sample surface and, subsequently, from the pores. This made it possible to visualize three-dimensional morphology of the frozen sample. All samples were observed with a low-vacuum secondary electron detector, using the accelerating voltage 30 kV. Lyophilized PHEMA slabs (Runs 3 and 8) filled with microspheres were also investigated by LVSEM; however, the microspheres were washed out of the pores during freezing and, consequently, they were scarcely observed on the micrographs.

High-vacuum scanning electron microscopy (HVSEM) was carried out with an electron microscope Vega TS 51355 (Tescan, Czech Republic). Permeability of the water-imbibed slabs (Runs 7 and 9) was determined by the flow of water suspension of the polymer microspheres. Before observation, the wet hydrogel slab was placed on a wet filtration paper and a droplet of a suspension of 8-μm PSt microspheres in water was put on the top. The sample was dried at ambient temperature and cut with a sharp blade in the direction of the microsphere flow. Samples showing the top, bottom and cross-sections of flowed-through slabs were sputtered with a 8-nm layer of platinum using a vacuum sputter coater (Baltec SCD 050), fixed with a conductive paste to a brass support and observed in a scanning electron microscope in high vacuum (10^{-3} Pa), using the acceleration voltage 30 kV and a secondary-electrons detector. This technique made it possible to observe both microspheres and pores of the hydrogel.

2.3.2. Solvent regain

The solvent (water or cyclohexane – CX) regain was determined in 1 × 2 cm sponge slabs kept for 1 week in deionized water, which was exchanged daily. Water regain was measured by two methods: (i) centrifugation [32] (WR_c) and (ii) suction (WR_s). In centrifugation method, solvent-swollen samples with imbibed solvent in glass columns with fritted disc were centrifuged at 980 g for 10 min and immediately weighed (w_w – weight of hydrated sample), then vacuum-dried at 80 °C for 7 h and again weighed (w_d – weight of dry sample). In the second method, excessive water was removed from swelled slab by suction and the slab weighted to determine w_w. Weight of the dry sample w_d was determined as above. Water regains WR_c or WR_s (ml/g) were calculated according to the equation:

$$WR_c(WR_s) = \frac{w_w - w_d}{w_d} \quad (1)$$

The results are average values of two measurements for each slab. To measure cyclohexane regain (CXR) by centrifugation, equilibrium water-swollen slabs were successively washed with ethanol, acetone and finally cyclohexane. Using the solvent-exchange method, a thermodynamically good (swelling) solvent in the swollen gel was replaced by a thermodynamically poor solvent (non-solvent). Porosity of the slabs (p) was calculated from the water and cyclohexane regains (Table 1) and PHEMA density ($\rho = 1.3$ g/ml) according to the equation:

$$p = \frac{R \times 100}{R + (1/\rho)}(\%) \quad (2)$$

where $R = WR_c$, WR_s, or CXR (ml/g).

2.3.3. Mercury porosimetry

Pore structure of freeze-dried PHEMA slabs was characterized on a mercury porosimeter Pascal 140 and 440 (Thermo Finigan, Rodano, Italy). It works in two pressure intervals, 0–400 kPa and 1–400 MPa, allowing determination of meso- (2–50 nm), macro- (50–1000 nm) and small superpores (1–116 μm). The pore volume and most frequent pore diameter were calculated under the assumption of a cylindrical pore model by the Pascal program using Washburn's equation describing capillary flow in porous materials [33]. The volumes of bottle and spherical pores were evaluated as the difference between the end values on the volume/pressure curve. Porosity was calculated according to Eq. (2), where cumulative pore volume (meso-, macro- and small superpores) from mercury porosimetry was used for R.

3. Results and discussion

3.1. Morphology of hydrogel slabs

The prepared PHEMA slabs had always an opaque appearance indicating a permanent porous structure. Pores are generally divided into micro-, meso-, macropore and small and large superpores. Morphology of water-swollen PHEMA slabs was investigated by LVSEM as shown in Fig. 1. Large 200–500 μm superpores were developed as imprints of NaCl crystals, which were subsequently washed out from the slab; the interstitial space between the pores was filled with the polymer. At the same time, ice crystals filling soft polymer net were clearly visible in the centre of the slab (Run 1, Table 1) prepared at the highest content of NaCl (41.4 vol.%) in the feed (Fig. 1a). The internal surface area was too small to be determined. Fig. 1b and c shows slabs from Runs 3 and 5 (40 and 37.9 vol.% NaCl), respectively, documenting their more compact structure accompanied by thicker walls between large superpores as compared with the slab from Run 1 (Fig. 1a). According to LVSEM, *ca.* 8-μm pores were observed in the walls between the large superpores, the presence of which was confirmed by mercury porosimetry (volume about 1 ml/g). Longitudinal cracks in the material structure (Fig. 1b and c) were obviously caused by sample handling and fast freezing in liquid nitrogen. Nevertheless, the LVSEM micrographs displayed only cross-sections of hydrogel slabs and it was not clear whether the hydrogel pores are interconnected.

Interconnection of pores is of vital importance for cell ingrowths in future applications to tissue regeneration. Pore interconnection was tested by the permeability of the whole slabs for different kinds of microspheres under two microscopic observations. Cross-sections of the frozen slabs filled with microspheres were first observed in LVSEM. The water-swollen slabs were also flowed through by a suspension of microspheres in water and their dried cross-sections were followed in HVSEM.

Slabs observed by LVSEM were immersed into water or a water suspension of the microspheres and frozen in liquid nitrogen. This preserved their water-swollen morphology. PHEMA (Run 3) prepared with neat NaCl (Fig. 2a) was compared with Run 8 obtained in the presence of NaCl together with a mixture of CyOH/DOH (Fig. 2d). Addition of liquid porogens did not change the morphology; however, it increased the pore volume (from 0.21 to 0.45 ml CX/g, Table 1) and softness of the slab. As a result, the slab had a tendency to disintegrate during the washing procedure. LVSEM micrographs of both PHEMA slabs filled with 2-μm ammonolyzed PGMA and 200–400 nm PANI microspheres is illustrated in Fig. 2b and e and Fig. 2c and f, respectively. The micrographs showed undistorted morphology of the frozen hydrogels, but just a few microspheres and/or their agglomerates. This was attributed to the fact that most of them were washed out during preparation of the sample for LVSEM.

Morphology of the PHEMA slabs flowed through by a suspension of microspheres was observed by HVSEM. Fig. 3 shows HVSEM micrographs of cross-sections of the top and bottom part of the slabs from Runs 3, 5 and 8 flowed through by a suspension of 8-μm sulfonated PSt microspheres in water. While the microspheres flowed through the slab from Run 3, they did not penetrate the slabs from Runs 5 and 8 prepared in the presence of a rather low content of NaCl (37.9 vol.%). At the same time, surface and inner structure of the slabs slightly differed. Fig. 4 shows HVSEM of the cross-section of the PHEMA slab obtained with cubic NaCl crystals as a porogen (Run 7). While Fig. 4a shows the bulk, panels b–d show detailed sections. Again, small superpores with an average size of about 13 μm were in the walls between the large superpores, forming small channels through which water flowed. To prove or exclude the interconnection of at least some pores, a suspension of 8-μm sulfonated polystyrene (PSt) microspheres in water was poured on the centre of the top side of the gel. While water flowed through the hydrogel bulk, the microspheres were retained on the surface of the hydrogel or penetrated only superficial layers due to

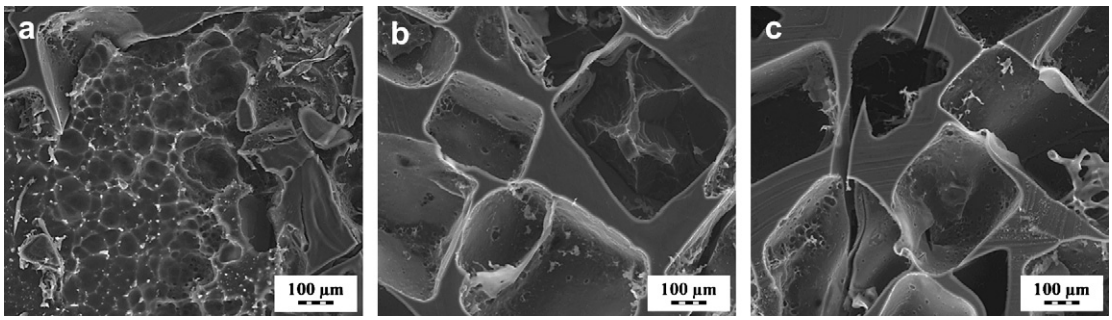

Fig. 1. LVSEM micrographs showing frozen cross-section of PHEMA slabs prepared with (a) 41.4 vol.% – Run 1, (b) 40 vol.% – Run 3, and (c) 37.9 vol.% NaCl (250–500 μm) – Run 5. PHEMA crosslinked with 2 wt.% EDMA (relative to monomers).

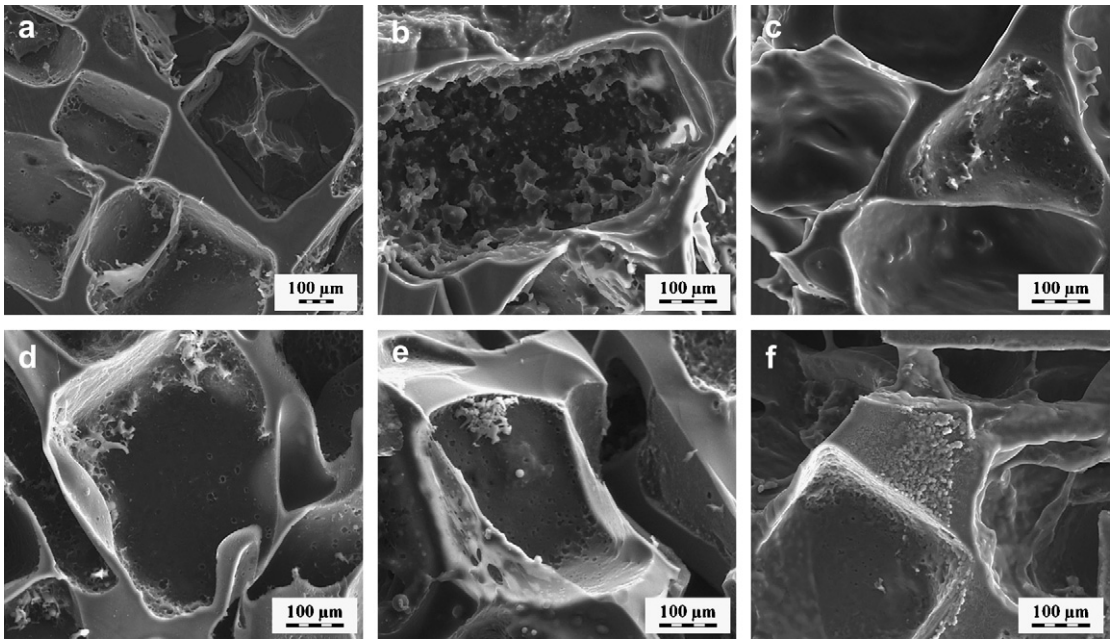

Fig. 2. LVSEM micrographs showing frozen cross-section of PHEMA slabs; (a–c) – Run 3; (d–f) – Run 8; (a and d) neat and filled with (b and e) 2-μm ammonolyzed PGMA and (c and f) 200–400 nm PANI microspheres.

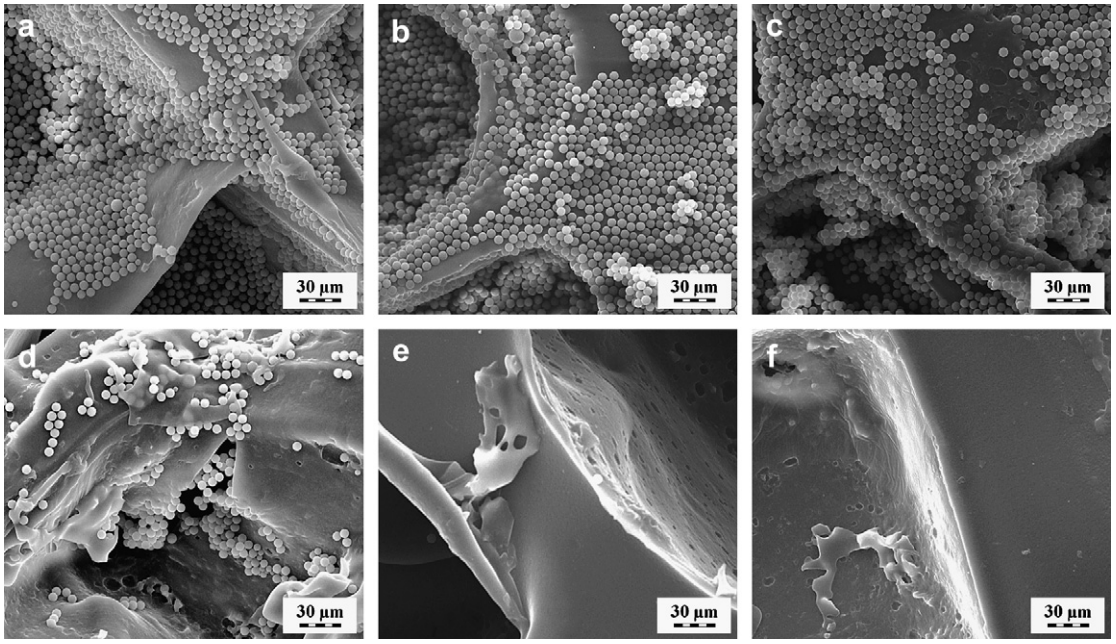

Fig. 3. HVSEM micrographs of PHEMA slabs; (a and d) – Run 3, (b and e) – Run 5 and (c and f) – Run 8 showing top (a–c) and bottom (d–f) of the hydrogels after the flow of a suspension of 8-μm sulfonated PSt microspheres in water.

the surface cracks (Fig. 4a and b). This confirmed that the pores of PHEMA slabs obtained with a low content of NaCl porogen (35.9 vol.%) did not communicate. In contrast, Fig. 5 presents cross-section of the PHEMA hydrogel from Run 9 (both bulk and detailed) obtained with needle-like $(NH_4)_2SO_4$ crystals as a porogen. This porogen allowed the formation of connected pores which is explained by the needle-like structure of ammonium sulfate crystals that are linked to the gel structure. At the same time, the crystals grew to large structures due to the presence of saturated $(NH_4)_2SO_4$ solution in the feed. As a result, long interconnected large superpores – channels – were formed. This is documented in Fig. 5a–d by the fact that suspension of 8-μm sulfonated PSt microspheres in water deposited in the centre of the top side of the hydrogel flowed through. The captured microspheres are well visible in Fig. 5b–d. They accumulated at the places of pore narrowing; their majority, however, was found on the bottom part of the hydrogel. In such a way, the flow of water suspension of microspheres in the hydrogel was traced.

Mechanical properties of the porous hydrogels were sensitive to the concentration of porogen in the feed. Slabs with lower contents of NaCl and therefore higher proportion of PHEMA had thicker walls between the pores and were more compact allowing increased swelling of polymer chains in water. Two PHEMA slabs with the highest contents of NaCl in the feed (41.4 vol.% – Run 1 and 40.8 vol.% – Run 2) possessing thin polymer walls between large superpores easily disintegrated.

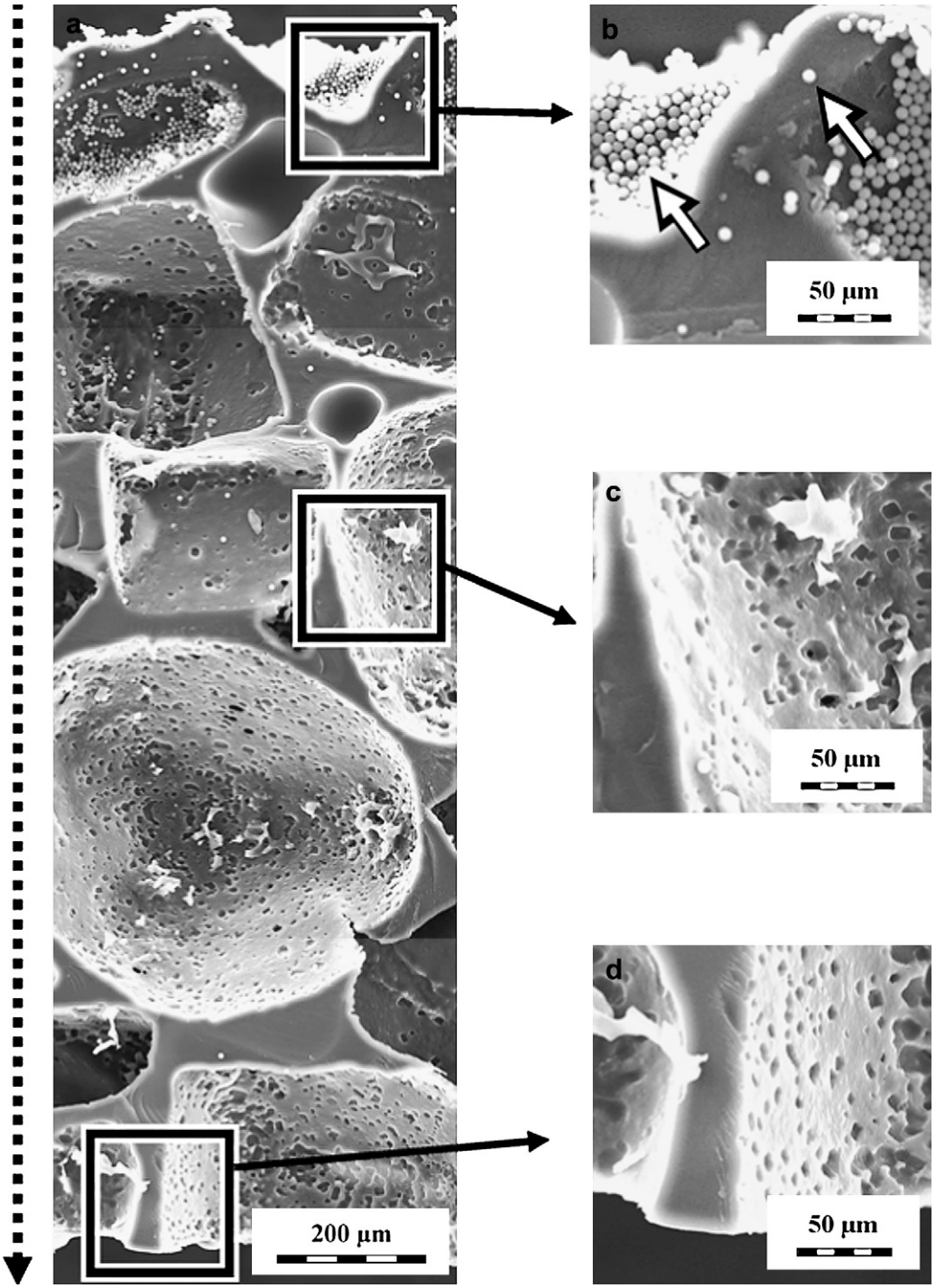

Fig. 4. Selected HVSEM micrographs showing cross-section of PHEMA slab 3 mm thick (Run 7) obtained with NaCl (250–500 μm) as a porogen after passing of a suspension of 8-μm sulfonated PSt microspheres in water (in the direction of the dotted line). (a) The whole cross-section through the slab and selected details from (b) top, (c) centre and (d) bottom. PSt microspheres are denoted with white arrows.

3.2. Characterization of porosity by solvent regain

Dependences of porosity of PHEMA slabs calculated from water or cyclohexane regain and also from mercury porosimetry on NaCl content in the polymerization feed showed similar behaviour (Fig. 6). Porosities of 81–91% for water regain were obtained by suction, 49–57% for water regain by centrifugation, 14–42% for cyclohexane regain and 31–70% for mercury porosimetry. The porosity determined by centrifugation of samples soaked with water and cyclohexane (solvents with different affinities to polar methacrylate chain) consists of two contributions: filling of the pores and swelling (solvation) of PHEMA chains. The uptake of cyclohexane, a thermodynamically poor solvent which cannot swell the polymer, is a result of the former contribution only, reflecting thus the pore volume. The porosities calculated from water regain and determined by centrifugation were therefore always higher than those from cyclohexane regain demonstrating thus swelling of polymer chains with water (Table 1). Solvent regains were affected by the concentration of NaCl porogen in the polymerization feed. Porosities according to both water and

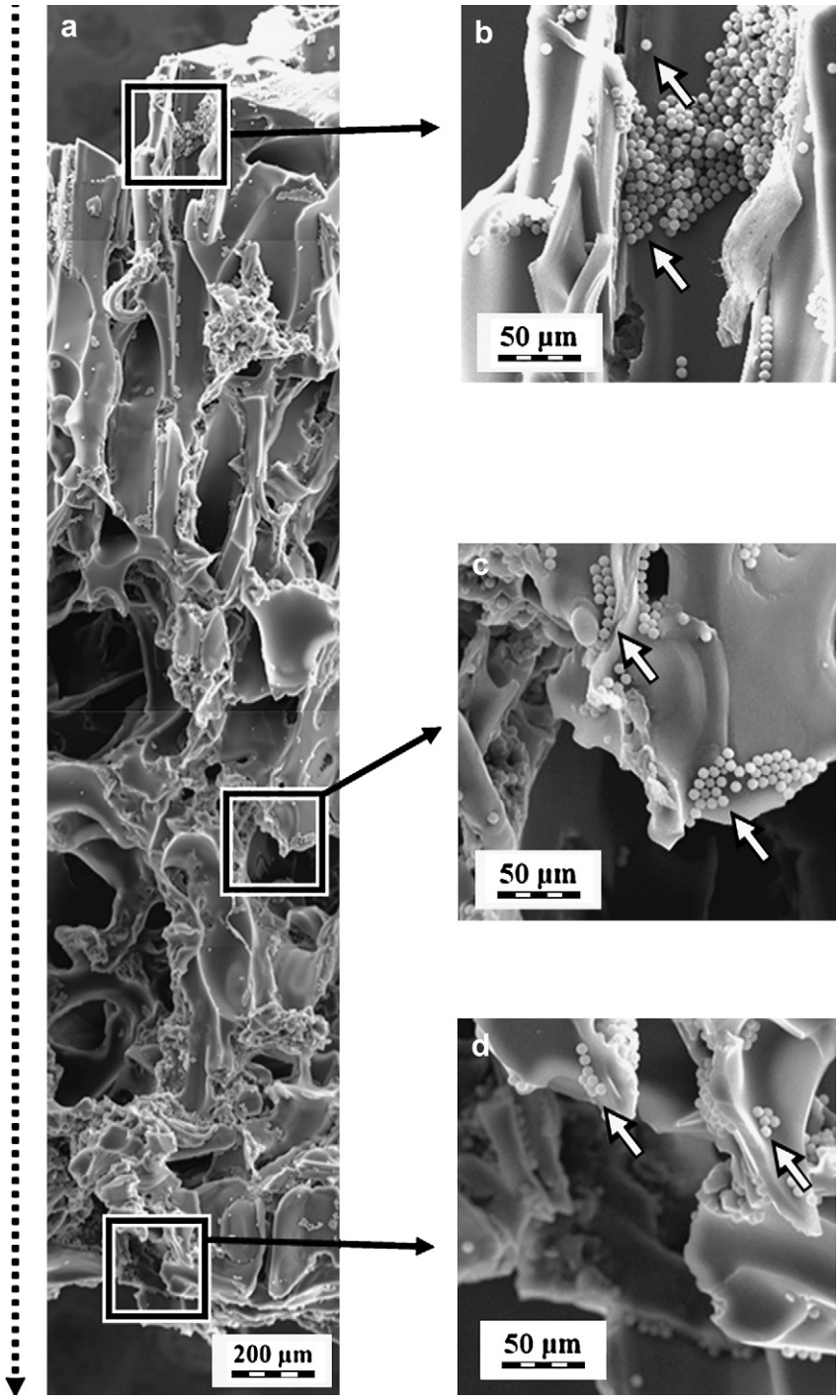

Fig. 5. Selected HVSEM micrographs showing cross-section of PHEMA slab 3 mm thick (Run 9) obtained with $(NH_4)_2SO_4$ (100 × 600 μm) as a porogen after passing of a suspension of 8-μm sulfonated PSt microspheres in water (in the direction of the dotted line). (a) The whole cross-section through the slab and selected details from (b) top, (c) centre and (d) bottom. PSt microspheres are denoted with white arrows.

cyclohexane regains determined by centrifugation slightly increased with increasing volume of NaCl porogen in the polymerization feed from 35.9 to 40 vol.% and then decreased with a further NaCl increase up to 41.4 vol.% (Fig. 6). In the latter range of NaCl, the porosity determined by mercury porosimetry exhibited an analogous dependence. This decrease in solvent and mercury regains can be explained by thin polymer walls between large superpores inducing collapse of the porous structure. In the concentration range of 35.9–40 vol.% NaCl in the feed, mercury porosimetry provided higher porosities than those obtained from water regain because centrifugation at 980 g obviously did not retain water in large superpores. Retained water reflected thus only small superpores, closed pores and solvation of the polymer in water similarly as observed earlier for macroporous PHEMA slabs [34]. Water regain was determined also by the suction method (Table 1) which gave the values several times higher (3.3–7.5 ml/g) than those determined by centrifugation because, in the former technique, water filled all the pores in the polymer structure, including large superpores, in contrast to the latter one. As expected, porosity determined by water regain by the suction method increased with increasing volume of NaCl porogen in the polymerization feed.

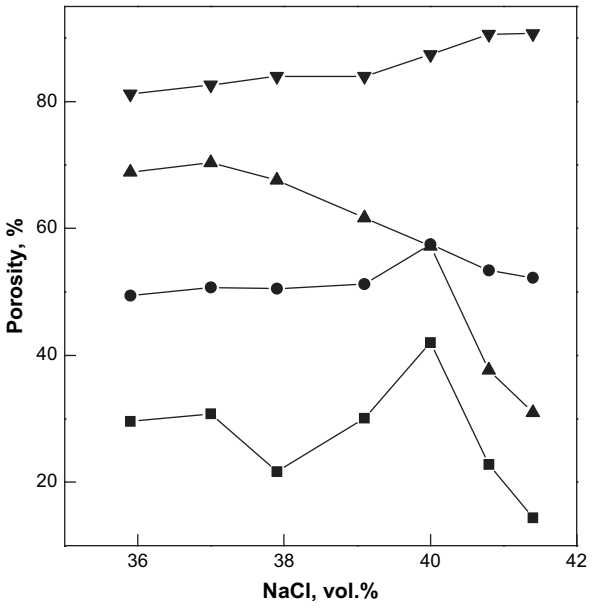

Fig. 6. Dependence of porosity of PHEMA slabs determined from cyclohexane (■) and water regain measured by centrifugation (●) or suction (▼) and mercury porosimetry (▲) on the content of NaCl (250–500 μm) porogen in the polymerization feed.

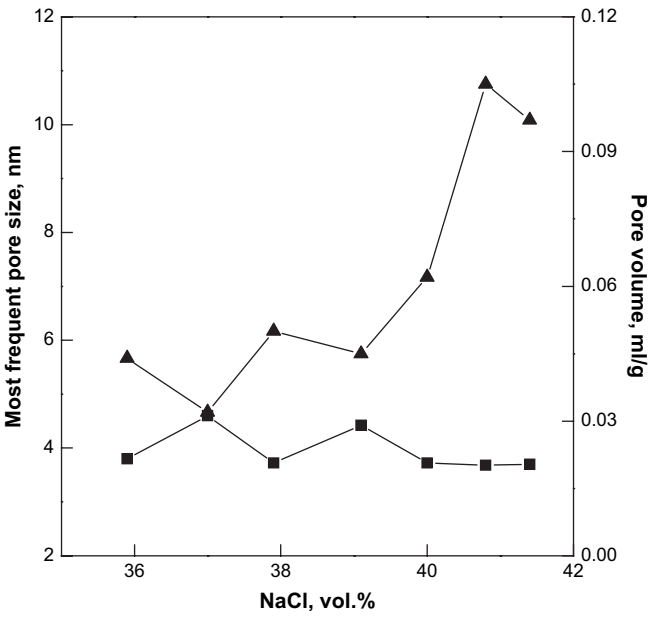

Fig. 7. Dependence of pore volume (▲) and most frequent mesopore size (■) of PHEMA slabs on the content of NaCl (250–500 μm) porogen in the polymerization feed according to mercury porosimetry.

The slab from Run 8 formed in the presence of NaCl and CyOH/DOH porogen showed higher solvent regains and mercury penetration than the comparable slab from Run 5 obtained with the same content of neat NaCl (Table 1). This can be explained by the higher total amount of porogen in the former slab. In contrast, the slab from Run 9 prepared with needle-like $(NH_4)_2SO_4$ crystals as a porogen had the lowest solvent and mercury regains of all the samples. The exception was water regain by centrifugation which was identical with that of sample (Run 1, Table 1) having a similar content of the NaCl porogen in the feed. This can imply that only large continuous superpores were present in this slab and small superpores, macro- and mesopores were almost absent as evidenced by the low values of solvent and mercury regains.

3.3. Characterization of porosity by mercury porosimetry

The advantage of mercury porosimetry consists in that it provides not only pore volumes, but also pore size distribution not available by other techniques. The method measures samples dried by lyophilization, which does not distort the pore structure. As already mentioned, porosities determined by mercury porosimetry were lower than those obtained from water regain by the suction method which included large superpores. The porosities were systematically higher than those from water and cyclohexane regains detected by centrifugation. This was due to better filling of the compact xerogel structures obtained at lower contents of NaCl in the feed with mercury under a high pressure than with water or cyclohexane under atmospheric pressure. Fig. 7 shows the dependence of most frequent mesopore size of PHEMA slabs and their pore volumes on the NaCl porogen content in the polymerization feed. Predominantly, 4–5 nm mesopores were detected with their volume increasing from 0.03 to 0.1 ml/g with increasing NaCl content in the polymerization feed. Macropores were absent and very low values of specific surface areas (<0.1 m^2/g) were found. The presence of CyOH/DOH porogen (Run 8) did not substantially affect the formation of meso- and macropores (volume 0.022 ml/g), because the amount of crosslinker in the polymerization feed was limited to only 2 wt.%. The separation of the polymer from the porogen phase could not thus occur and porous structure was not formed. Both in hydrophobic styrene–divinylbenzene [35,36] and polar methacrylate copolymers [37] prepared in the presence of liquid porogens, phase separation and formation of macroporous structure occurred at crosslinker contents higher than 10 wt.%.

Fig. 8 represents the dependence of most frequent small superpore size of PHEMA slabs and their pore volume on the content of NaCl porogen in the polymerization feed. Pore size increased up to 28–69 μm with increasing NaCl volume. This was pronounced in the range 40–41.4 vol.% NaCl probably due to the aggregation of NaCl crystals in the mixture at their high contents. All the investigated samples contained small superpores, the volume of which was about 20 times higher than that of mesopores. The volume of small superpores continuously decreased from 1.8 to 0.2 ml/g with increasing NaCl amount in the feed. This could be explained

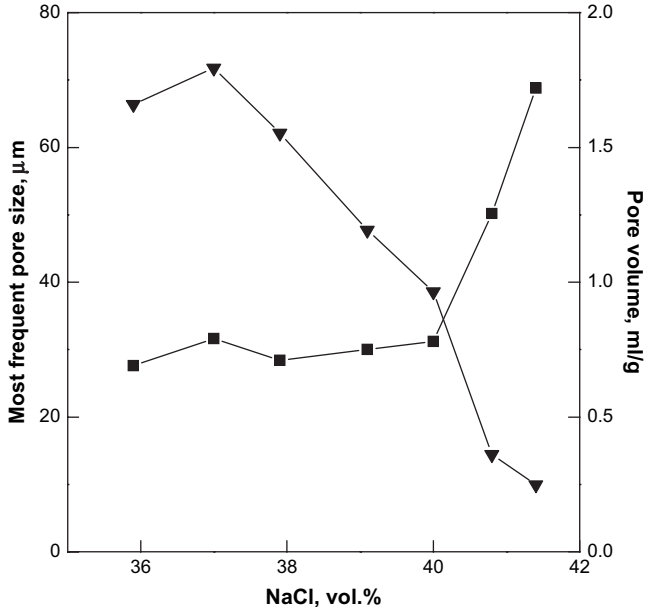

Fig. 8. Dependence of pore volume (▼) and most frequent small superpore size (■) of PHEMA slabs on the content of NaCl (250–500 μm) porogen in the polymerization feed according to mercury porosimetry.

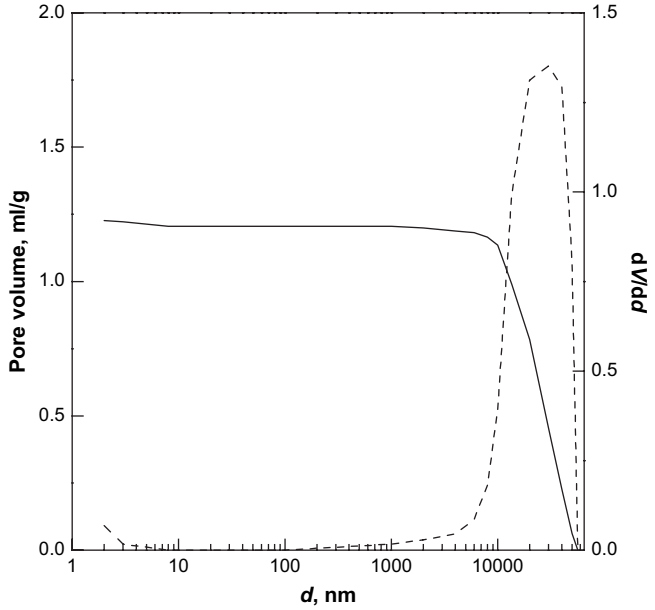

Fig. 9. Cumulative pore volume (—) and pore size distribution (- - -) of the Run 4 slab determined by mercury porosimetry in the range 1.88–116 μm.

by collapse of the pore structure and destruction of last two slabs with the highest content of NaCl porogen (Runs 1 and 2) under high pressure as mentioned above. The size of small superpores according to mercury porosimetry was by an order of magnitude smaller than the particle size of the used NaCl porogen (250–500 μm) because the method was able to detect the superpores only in the size range 1–116 μm (Fig. 9). Large superpores (imprints of NaCl crystals) were detected by LVSEM. Fig. 9 exemplifies a typical cumulative pore volume and a derivative pore size distribution curve of PHEMA (Run 4) with a decisive contribution of small superpores of 25 μm in size.

4. Conclusions

Superporous PHEMA slabs were prepared by bulk radical copolymerization of HEMA and EDMA in the presence of NaCl or $(NH_4)_2SO_4$ crystals. Morphology of the prepared slabs was characterized by several methods including scanning electron microscopy both in swollen (LVSEM) and dry (HVSEM) states, solvent (water and cyclohexane) regains, high- and low-pressure mercury porosimetry of lyophilized samples and dynamic desorption of nitrogen. Morphology and porous structure of the slabs were preferentially affected by the character and amount of the used porogen – NaCl or $(NH_4)_2SO_4$. After washing out of the salts from PHEMA, three types of pores were detected by microscopic and mercury porosimetry methods, including large superpores (hundreds of micrometers) as imprints of salt crystals. The slabs can be divided into two groups, with disconnected and interconnected pores. The latter allowed the passage of suspension of microspheres in water, which was observed only for the sample with ammonium sulfate crystals used as a porogen and the samples with the highest content of NaCl in the feed. Interconnected pores are crucial for potential application of the slabs as living cell supports. LVSEM showed the undistorted (frozen) structure of the hydrogels, but only few flowed-through microspheres could be observed as they tended to escape from the pores during sample preparation. HVSEM seemed to be the best microscopic technique especially for the observation of permeability of hydrogel slabs to 8-μm microspheres. Slabs were initially flowed through by the microspheres in their natural wet state, but the specimens were dried before SEM observation. The microspheres could be traced both on the upper/lower parts of the slabs and on the cross-sections.

Mercury porosimetry provided detailed description of morphology of PHEMA slabs with pore sizes from units of nanometers to tens of micrometers. The drawback of the method is that the slabs are not measured in the swollen, but dry state, as xerogels. But comparison of the data in both wet and dry states showed that lyophilization did not change the pore structure. The mesopores and small superpores detected by mercury porosimetry cannot be formed by the imprinting mechanism. While mesopores present only in very small amounts may be formed by phase separation, small superpores arise by polymer contraction in the walls of large superpores. Small 28–69 μm superpores were mainly present in the porous structure apart from the large superpores (imprints of solid porogen crystals), the volume of which was several times higher than that of other pores, as confirmed by water regain obtained by the suction method.

Acknowledgement

Financial support of the EU Grant Artemis (LSHM-CT-2007-037862) is gratefully acknowledged.

References

[1] Kofron MD, Cooper JA, Kumbar SG, Laurencin CT. Novel tubular composite matrix for bone repair. J Biomed Mater Res Part A 2007;82:415–25.
[2] Moroni L, Hendriks JAA, Schotel R, De Wijn JR, Van Blitterswijk CA. Design of biphasic polymeric 3-dimensional fiber deposited scaffolds for cartilage tissue engineering applications. Tissue Eng 2007;13:361–71.
[3] Dvořánková B, Holíková Z, Vacík J, Königová R, Kapounková Z, Michálek J, et al. Reconstruction of epidermis by grafting of keratinocytes cultured on polymer support – clinical study. Int J Dermatol 2003;42:219–23.
[4] Bhang SH, Lim JS, Choi CY, Kwon YK, Kim BS. The behavior of neural stem cells on biodegradable synthetic polymers. J Biomater Sci Polym Ed 2007;18:223–39.
[5] Bianchi F, Vassalle C, Simonetti M, Vozzi G, Domenici C, Ahluwalia A. Endothelial cell function on 2D and 3D micro-fabricated polymer scaffolds: applications in cardiovascular tissue engineering. J Biomater Sci Polym Ed 2006;17:37–51.
[6] Sander EA, Alb AM, Nauman EA, Reed WF, Dee KC. Solvent effects on the microstructure and properties of 75/25 poly(D,L-lactide-*co*-glycolide) tissue scaffolds. J Biomed Mater Res Part A 2004;70:506–13.
[7] Nam YS, Yoon JJ, Park TG. A novel fabrication method of macroporous biodegradable polymer scaffolds using gas foaming salt as a porogen additive. J Biomed Mater Res Part B Appl Biomater 2000;53:1–7.
[8] Kroupová J, Horák D, Pacherník J, Dvořák P, Šlouf M. Functional polymer hydrogels for embryonic stem cell support. J Biomed Mater Res Part B Appl Biomater 2006;76:315–25.
[9] Tighe B, Corkhill P. Hydrogels in biomaterials design: is there life after poly-HEMA? Macromol Rep 1994;A31:707–13.
[10] Plieva FM, Galaev IY, Mattiasson B. Macroporous gels prepared at subzero temperatures as novel materials for chromatography of particulate-containing fluids and cell culture applications. J Sep Sci 2007;30:1657–71.
[11] Mooney DJ, Baldwin DF, Suh NP, Vacanti JP, Langer R. Novel approach to fabricate porous sponges of poly(D,L-lactic-*co*-glycolic acid) without the use of organic solvents. Biomaterials 1996;17:1417–22.
[12] Chung HJ, Park TG. Surface engineered and drug releasing pre-fabricated scaffolds for tissue engineering. Adv Drug Delivery Rev 2007;59:249–62.
[13] Ferreira LS, Gerecht S, Fuller J, Shieh HF, Vunjak-Novakovic G, Langer R. Bioactive hydrogel scaffolds for controllable vascular differentiation of human embryonic stem cells. Biomaterials 2007;28:2706–17.
[14] Tangsadthakun C, Kanokpanont S, Sanchavanakit N, Pichyangkura R, Banaprasert T, Tabata Y, et al. The influence of molecular weight of chitosan on the physical and biological properties of collagen/chitosan scaffolds. J Biomater Sci Polym Ed 2007;18:147–63.
[15] Wachiralarpphaithoon C, Iwasaki Y, Akiyoshi K. Enzyme-degradable phosphorylcholine porous hydrogels cross-linked with polyphosphoesters for cell matrice. Biomaterials 2007;28:984–93.
[16] Treml H, Woelki S, Kohler HH. Theory of capillary formation in alginate gels. Chem Phys 2003;293:341–53.
[17] Konno T, Ishihara K. Temporal and spatially controllable cell encapsulation using a water-soluble phospholipid polymer with phenylboronic acid moiety. Biomaterials 2007;28:1770–7.
[18] Heckmann L, Schlenker HJ, Fiedler J, Brenner R, Dauner M, Bergenthal G, et al. Human mesenchymal progenitor cell responses to a novel textured poly(L-lactide) scaffold for ligament tissue engineering. J Biomed Mater Res Part B Appl Biomater 2007;81:82–90.

[19] Darling AL, Sun W. 3D microtomographic characterization of precision extruded poly-ε-caprolactone scaffolds. J Biomed Mater Res Part B Appl Biomater 2004;70:311–7.
[20] Rhee W, Rosenblatt J, Castro M, Schroeder J, Rao PR, Harner CFH, et al. In vivo stability of poly(ethylene glycol)–collagen composites. In: Harris JM, Zalipsky S, editors. Poly(ethylene glycol) chemistry and biological applications. ACS symposium series, vol. 680; 1997. p. 420–40.
[21] Savina IN, Galaev IY, Mattiasson B. Ion-exchange macroporous hydrophilic gel monolith with grafted polymer brushes. J Mol Recognit 2006;19:313–21.
[22] Carampin P, Conconi MT, Lora S, Menti AM, Baiguera S, Bellini S, et al. Electrospun polyphosphazene nanofibers for in vitro rat endothelial cells proliferation. J Biomed Mater Res Part A 2007;80:661–8.
[23] Zhang CH, Zhang N, Wen XJ. Synthesis and characterization of biocompatible, degradable, light-curable, polyurethane-based elastic hydrogels. J Biomed Mater Res Part A 2007;82:637–50.
[24] Castner DG, Ratner BD. Biomedical surface science: foundation to frontiers. Surf Sci 2002;500:28–60.
[25] Lee KY, Mooney DJ. Hydrogels for tissue engineering. Chem Rev 2001;101:1869–79.
[26] Refojo MF. Hydrophobic interactions in poly(2-hydroxyethyl methacrylate) homogeneous hydrogel. J Polym Sci Part A1 Polym Chem 1967;5:3103–8.
[27] Ratner BD, Hoffman AS. Hydrogels for medical and related applications. ACS Symp Ser 1976;31:1–36.
[28] Horák D, Dvořák P, Hampl A, Šlouf M. Poly(2-hydroxyethyl methacrylate-*co*-ethylene dimethacrylate) as a mouse embryonic stem cell support. J Appl Polym Sci 2003;87:425–32.
[29] Horák D, Kroupová J, Šlouf M, Dvořák P. Poly(2-hydroxyethyl methacrylate)-based slabs as a mouse embryonic stem cell support. Biomaterials 2004;25:5249–60.
[30] Horák D, Shapoval P. Reactive poly(glycidyl methacrylate) microspheres prepared by dispersion polymerization. J Polym Sci Part A Polym Chem 2000;38:3855–63.
[31] Stejskal J, Kratochvíl P, Gospodinova N, Terlemezyan L, Mokreva P. Polyaniline dispersions: preparation of spherical particles and their light-scattering characterization. Polymer 1992;33:4857–8.
[32] Štamberg J, Ševčík S. Chemical transformations of polymers III. Selective hydrolysis of a copolymer of diethylene glycol methacrylate and diethylene glycol dimethacrylate. Collect Czech Chem Commun 1966;31:1009–16.
[33] Porosimeter Pascal 140 and Pascal 440, Instruction manual; 1996. p. 8.
[34] Hradil J, Horák D. Characterization of pore structure of PHEMA-based slabs. React Funct Polym 2005;62:1–9.
[35] Millar JA, Smith DG, Marr WE, Kresmann TRE. Solvent modified polymer networks. Part 1. The preparation and characterization of expanded-networks and macroporous styrene–DVB copolymers and their sulfonates. J Chem Soc 1963:218–25.
[36] Kun KA, Kunin R. Macroreticular resins III. Formation of macroreticular styrene–divinylbenzene copolymers. J Polym Sci Part A1 Polym Chem 1968;6:2689–701.
[37] Hradil J, Křiváková M, Starý P, Čoupek J. Chromatographic properties of macroporous copolymers of 2-hydroxyethyl methacrylate and ethylene dimethacrylate. J Chromatogr 1973;79:99–105.